Available online at www.sciencedirect.com
SCIENCE DIRECT®
Journal of Crystal Growth 275 (2005) 504–511
JOURNAL OF CRYSTAL GROWTH
www.elsevier.com/locate/jcrysgro

Zone-levelling Czochralski growth of MgO-doped near-stoichiometric lithium niobate single crystals

C.B. Tsai[a], Y.T. Hsia[a], M.D. Shih[a], C.Y. Tai[a], C.K. Hsieh[b], W.C. Hsu[b], C.W. Lan[a,*]

[a]*Department of Chemical Engineering, National Taiwan University, Taipei, Taiwan 10617, ROC*
[b]*Sino-American Silicon Product Inc., Hsinchu, Taiwan*

Received 20 October 2004; accepted 6 December 2004
Communicated by D.T.J. Hurle
Available online 19 January 2005

Abstract

The zone-levelling Czochralski (ZLCz) technique was used to grow MgO-doped near-stoichiometric lithium niobate (SLN) crystals for the first time. The crystal was pulled from a Li-rich solution (58–60 mol% of Li_2O) having an SLN solid supplied from below in a slender platinum crucible. An inner crucible was also used to avoid bubble incorporation. With 1 mol% MgO doping, three inclusion-free SLN crystals were grown. The transmittance along the grown crystals was found satisfactory ($76\pm1\%$) having an absorption edge of 303 ± 1 nm. The small variation of the composition ($Li/Nb = 0.975\pm0.005$ and $Mg/Nb = 1.07\pm0.02$ mol%), refractive indices ($n_o = 2.286\pm0.0005$ and $n_e = 2.189\pm0.0007$), and the Curie temperature ($1209.5\pm1.5\,^{\circ}C$) further confirm ZLCz as a proven method for growing SLN single crystals.

PACS: 81.10.−h; 61.72.Ss; 42.70.Mp

Keywords: A1. Characterization; A1. Segregation; A2. Zone-levelling Czochralski method; B1. Growth from solutions; B1. Lithium niobate; B2. Nonlinear optic materials

1. Introduction

Lithium niobate ($LiNbO_3$, LN) is an important material for various optical applications, such as second-harmonic generation, optical switches, optical modulators, and holographic storage devices [1–3]. Through quasi-phase matching (QPM), the crystal with periodical poling (PPLN) has shown superior properties and opens its new era for applications [4]. However, because the ionic bonding of Nb/O is much stronger than that of Li/

*Corresponding author. Tel/fax: +886 2 2363 3917.
E-mail address: cwlan@ntu.edu.tw (C.W. Lan).

0022-0248/$ - see front matter © 2004 Elsevier B.V. All rights reserved.
doi:10.1016/j.jcrysgro.2004.12.026

O, the Li/Nb ratio at the congruent composition (referred as CLN) is smaller than unity being about 48.4/51.6 [5]. This nonstoichiometry introduces anti-site defects, where the lithium ion sites are occupied by the niobium ions. The intrinsic defects result in high internal electric fields and stronger photorefractive damage in laser applications [6]. With MgO doping up to 5 mol%, the photoresistance of CLN can be significantly enhanced. Even so, the most straightforward way to enhance the properties is to grow near-stoichiometric lithium niobate (SLN) from a Li-rich solution [7,8]. For SLN crystals, a small amount of MgO doping (1 mol%) has enhanced significantly the laser damage threshold up to 2 MW/cm^2 [6].

Pulling an SLN crystal from a Li-rich (self-flux) solution by the Czochralski method is not practical due to the segregation problem. Adding K_2O to the flux solution has been found feasible [9]. However, the growth rate for getting an inclusion-free crystal is usually very slow, less than about 0.2 mm/h [10], and this limits its commercial applications. Apparently, to grow an SLN crystal with a good yield, a continuous process is necessary. The first successful continuous method to grow SLN crystal is the double crucible Czochralski method (DCCz) [11,12]. In this method, the crystal is grown from a Li-rich (58–60 mol% Li_2O) solution in the inner crucible, and the stoichiometric powder is continuously fed into the outer crucible according to the mass pulling rate of the growing crystal. Although DCCz is a useful process for SLN growth, the powder feeding requires a complicate design, and this is not convenient for a conventional Czochralski puller. A very similar process proposed by Kan et al. is also called the double crucible Czochralski method, but with solution feeding [13]. In this method, instead of powder feeding, the continuous feeding is done by lifting the outer crucible during crystal pulling. Unfortunately, the growth was not successful due to the mixing of the solutions between the inner and outer crucibles.

In this report, a novel zone-levelling Czochralski (ZLCz) technique is proposed to grow SLN single crystals. This technique, as shown in Fig. 1a, is a combination of the zone melting and Czochralski

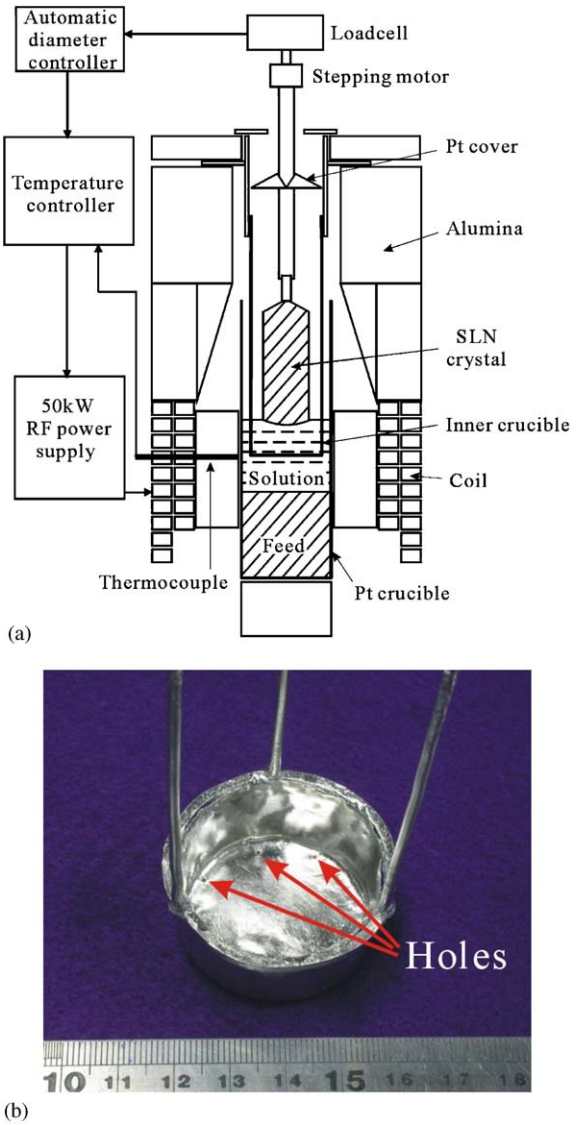

Fig. 1. (a) Schematic diagram of the zone-levelling Czochralski method with an ADC system; (b) platinum inner crucible.

methods. During crystal pulling, the stoichiometric solid material is continuously fed from below by lifting the crucible. Also, the composition of the Li-rich solution is the same as that used in DCCz for growing SLN crystals. However, with the solid feeding, bubble formation was found inevitable [14]. To avoid bubble incorporation, an inner crucible with small holes (as shown in

Fig. 1b) needs to be used. As will be illustrated shortly, for the growth of MgO-doped SLN, the composition uniformity could be easily obtained during steady-state growth. In Section 2, experimental procedures are described. Section 3 is devoted to results and discussion, followed by conclusions in Section 4.

2. Experimental procedure

Powder Nb_2O_5 (99.995% purity, Taki Chemical Co.), Li_2CO_3 (99.995% purity, Honjo chemical Co.) and MgO (99.9% purity, Sigma-Aldrich, Inc.) were used as raw materials. They were first mixed at appropriate proportions in a ball mill for 24 h, and then pressed into several blocks ($\varnothing$ 5 cm × 5 cm) by using a hydraulic press at a pressure of 100 kg/cm^2. The pressed powder was calcined and sintered at 1000 °C for 24 h. A much denser feeding material was required to avoid the formation of big bubbles during the SLN crystal growth.

The stoichiometric blocks were filled into a 15.5 cm long platinum crucible ($\varnothing$ 5 cm with 1 mm in thickness) and melted by RF induction heating. After the molten zone was stabilized, a much denser stoichiometric feed was prepared by directional solidification with a fast crucible translation speed (>10 mm/h) to avoid macro-segregation. The Li-rich (60 mol% Li_2O) block was then placed upon the feed material. Then, the outer crucible was lowered down to a given position, and the inner crucible was placed. The solution zone was gradually melted by lifting the crucible upward until the inner crucible was immersed to a proper position; the solution zone was controlled to be about 40–45 mm. The inner crucible is shown in Fig. 1b. It was made of platinum with 4 cm in diameter, 2 cm in height, and 0.1 mm in thickness. Eight small holes (0.5 mm in diameter) were punched at the bottom edge of the inner crucible to allow the solution to flow through. The use of the inner crucible was found necessary to grow bubble-free crystals. After the system was stabilized, a *c*-axis seed was carefully dipped into the solution to start the growth. During crystal growth, the crystal diameter was controlled by an automatic diameter control (ADC) system, where the crystal weight was measured and used for control. The schematic diagram of the feedback control is also illustrated in Fig. 1a. After the crystal diameter reached 15 mm, the outer crucible was lifted at a preset speed to feed the material. At the tailing stage, the outer crucible was stopped. The seed was rotated at 6 rpm and the pulling rate was 0.3–0.6 mm/h. Depending on the crystal pulling rate and the crystal diameter (20 or 22 mm), the feeding rate was adjusted from 0.05 to 0.12 mm/h. The hot zone used for crystal growth is sketched in Fig. 1a. With a suitable thermal configuration, the temperature gradient along the crystal could be controlled under 20 °C/cm, and this was found necessary to avoid crystal cracking.

After the crystal was detached from the solution zone, the outer crucible was lowered slowly to separate the inner crucible from the solution. Then, the crystal was cooled slowly for 24 h before harvesting. The grown crystal was annealed at 1000 °C for 16–24 h to release thermal stress. With the present zone composition (60 mol% Li_2O), the grown crystal was covered by some Li_3NbO_4, but it could be easily removed by an HF solution. The as-grown boule was oriented and then sliced into several wafers perpendicular to the *c*-axis. The wafers were lapped and polished to 1 mm in thickness for optical measurements.

The transmittance and absorbance of the wafers (1 mm in thickness) were measured by a JASCO V-570 UV–Visible–NIR Spectrometer. The cutoff wavelength was determined at the absorption coefficient of 20 cm^{-1}. The Curie temperature of the crystals was measured by a DSC (Netzsch Instrument HT-DSC 404). The ordinary (n_o) and extraordinary (n_e) refractive indices of the wafers were measured by a prism coupler (Metricon Model 2010) using a He–Ne laser as the light source (632.8 nm). To determine the Li/Nb ratio and the MgO content of the grown crystals, an ICP-AES (Jarrell–Ash ICAP 9000) was used; Li and Nb were determined separately.

3. Results and discussion

Three SLN crystals (20 to 22 mm in diameter and 50 to 100 mm in length) were grown

from a Li-rich solution by the ZLCz technique based on the same charge. The as-grown crystals are shown in Fig. 2. The crystal diameter was under good control by using our ADC system. However, the crystal surface was covered by a thin layer of Li_3NbO_4. After etched with HF, the crystals were transparent, but slightly yellow in color due to impurities. The 1st and the 3rd crystals were ended with the tailing process. However, to view the growing interface and to have a steady zone composition for the 3rd crystal to start with, the 2nd crystal was suddenly detached from the solution. As shown by the detached shape in Fig. 2, the growth interface was convex to the solution, and it was consistent with the one in the DCCz method [15].

Fig. 3 shows the variation of the zone temperature and the power during crystal growth of the 3rd crystal; the thermocouple position is shown in Fig. 1a. As shown, at the shouldering stage, both temperature and heating power were increasing. This is quite different from the traditional melt pulling that the power is decreased to enlarge the crystal size. This unique nature of the ZLCz crystal

Fig. 2. As-grown SLN single crystals by the ZLCz method. Crystals from left to right are the 1st, 2nd, and the 3rd crystals grown from the same solution zone; the growth speed was 0.3 mm/h for the 1st and the 2nd crystals and 0.6 mm/h for the 3rd crystals.

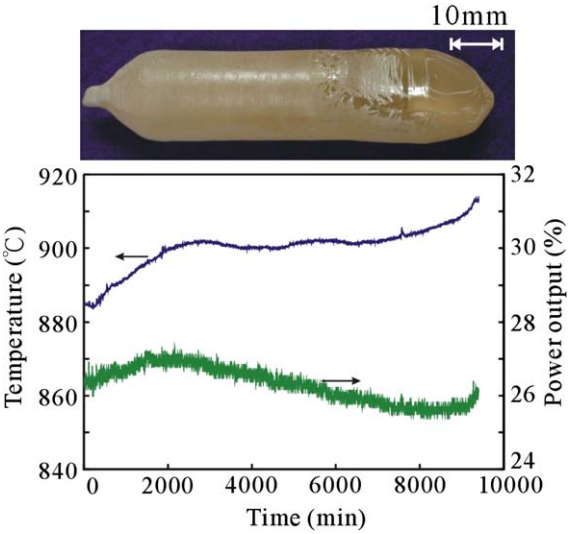

Fig. 3. Histories of power and zone temperature during the growth of the 3rd crystal.

pulling was a result of mass and energy transports. As the growth started, the composition gradients in the solution zone were built up gradually. Meanwhile, the zone position was adjusted by the power to enlarge the growing crystal. As shown in Fig. 3, it took about 2 cm in the growth distance to reach a steady state, i.e., both solutal and thermal fields stabilized. Then, the growth temperature remained stable and the heating power decreased gradually. The decreasing power was mainly caused by the decreasing heat loss from the crucible below the insulation zone as a result of the crucible lifting. Therefore, in order to keep the position of the solution/feed interface as stable as possible, as shown in Fig. 1a, no insulation was used below the heating zone to increase the axial thermal gradient. Finally, at the tailing stage, since the crucible lifting was stopped, the thermal behavior was the same as the traditional Cz pulling, i.e., both the power and the temperature increased.

To examine the quality of the grown crystals, the transmittances of the polished wafers were measured. Fig. 4 shows the comparison of the transmittance of the wafers sampled from different positions of the 2nd crystal. The transmittances of

the wafers were about 76% in the wavelength range of 450–800 nm. The deviations among the wafers were less than 2%. Other crystals also have similar transmittance spectra.

Important information for the stoichiometry of the grown crystals could also be drawn from the absorption edge, or the so-call cutoff wavelength, of the transmittance data. The cutoff value strongly depends on the Li/Nb ratio and the amount of dopants [16,17]; both factors reduce the cutoff wavelength. The distributions of the cutoff wavelength along the growth axis of the grown crystals are shown in Fig. 5. As shown, the deviation was only about ± 0.3 nm along the steadily grown body. The overall cutoff values

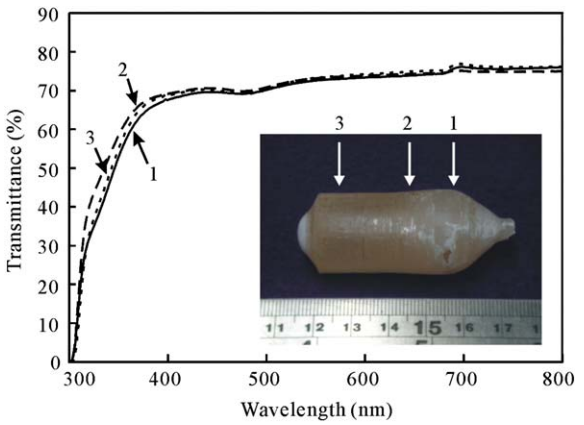

Fig. 4. Transmittances of the wafers cut from the 2nd crystal.

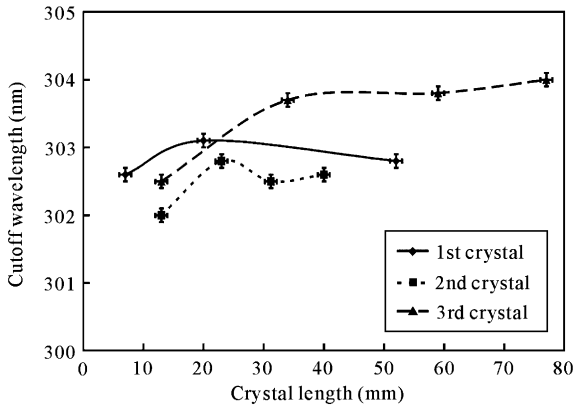

Fig. 5. Axial distributions of the cutoff wavelength of the grown crystals.

were within 303 ± 1 nm, and agreed well with the reported values: 304 nm for 0.78 mol% MgO-doped SLN and 300.8 nm for 1.98 mol% MgO-doped SLN in Ref. [16], and 302.5 nm for 0.6 mol% MgO-doped SLN and 301.5 nm for 1.8 mol% MgO-doped SLN in Ref. [18]. In addition, in a very recent paper [19], the 1 mol% MgO-doped SLN crystal grown from a solution with 11 mol% K_2O flux showed a slightly higher cutoff wavelength at about 305 nm. For a typical CLN wafer, the cutoff wavelength is about 320 nm. With 5 mol% MgO doping, the cutoff wavelength is reduced to about 308 nm [20]. According to Ref. [17], the difference of 1 nm in the cutoff wavelength corresponds to the change of 0.1 mol% in the $Li_2O/(Li_2O + Nb_2O_5)$ ratio. This implies that the 2 nm difference in our absorption edges among the crystals could be caused by the 1% difference in the Li/Nb ratio. The wafers from the 3rd crystal had higher cutoff wavelengths indicating that they might have lower Li/Nb ratios. This is believed to be due to the lower solution/feed interface, i.e., having a larger solution zone (dilution), due to less radiation heat loss from the outer crucible. In the first two growths, the crucible length below the insulation zone was changed from 3.6 to 2.8 cm and then to 2 cm, respectively, which meant that the area reduction for radiation heat loss was lower than 30% during the growth. However, in the third growth, the crucible length below the insulation zone was changed from 2 to 0.5 cm during the growth. This corresponded to an area reduction for radiation heat loss up to 75% during the growth. Furthermore, if we examine Fig. 5 again, the tail value of the 2nd crystal happened to be quite close to the head value of the 3rd crystal. And this was due to the sudden detachment of the 2nd crystal without the segregation coming from the tailing procedure. On the other hand, because of the tailing procedure (without crucible lifting) of the 1st crystal growth, some deviation could be found between the last point of the 1st crystal and the first point of the 2nd crystal.

Similar results were also observed in the refractive indices measurements, as shown in Fig. 6. The ordinary index and extraordinary index of the as-grown crystal were within

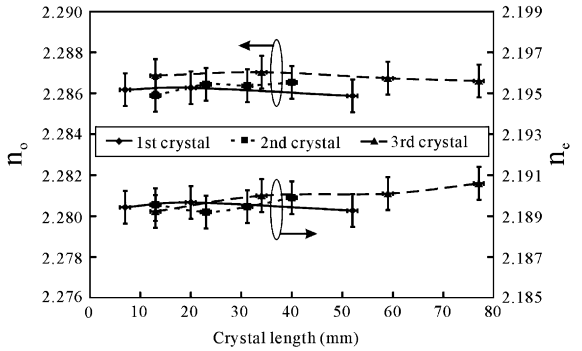

Fig. 6. Axial distributions of refractive indices of the grown crystals.

2.286 ± 0.0005 and 2.189 ± 0.0007, respectively. The 3rd crystal also had larger values of n_e. These values are also quite close to the reported ones; $n_o = 2.2865$ and $n_e = 2.1898$ for 1 mol% MgO-doped SLN [6] ($n_e = 2.189 \pm 0.0004$ for undoped SLN [21,22]). The higher n_e values also indicate lower Li/Nb ratios [6].

Beside the optical properties, the Curie temperature is also affected significantly by the stoichiometry and dopants. The dependence of the Curie temperature on the Li/Nb ratio (undoped) could be obtained from O'Bryan equation [23]. The effect of MgO doping was also studied extensively [16,24]. The distributions of the Curie temperatures of the 1st and the 3rd crystal are shown in Fig. 7. The obtained Curie temperatures were in good agreement with the reported values: 1206 °C for 0.78 mol% MgO-doped SLN and 1213 °C for 1.98 mol% MgO-doped SLN in Refs. [16,24]. From the measurements, both crystals showed a good axial uniformity. The slightly lower Curie temperatures observed in the 3rd crystal also implied the lower Li/Nb ratio, and this was consistent with the previous optical measurements. The deviation in the Curie temperature among our crystals was about 3 °C. According to O'Bryan equation [23], this deviation corresponds to about 0.5% difference in the Li/Nb ratio.

Although the previous measurements are believed to be more reliable than chemical analyses, we still measured the Li/Nb ratio and the MgO content along the 1st crystal for comparison. As shown in Fig. 8, the Li/Nb ratio was found within 0.975 ± 0.005, indicating about 1% deviation on the stoichiometry along the crystal; the deviation was comparable to the standard deviation of the measurement errors. On the other hand, the Mg concentration in the crystal was about 1.07 ± 0.02 mol% of Nb. Both results further indicated the good uniformity of the grown crystal. The composition of the starting and the final compositions of the solution zone were further measured. The Li/Nb ratio of the starting material was 1.487 (59.8 mol% Li_2O), and the final solution (after pulling out the 3rd crystal) was 1.44 (59 mol% Li_2O). The Mg/Nb ratio at the beginning and the end was close to 1.0 mol%. If we

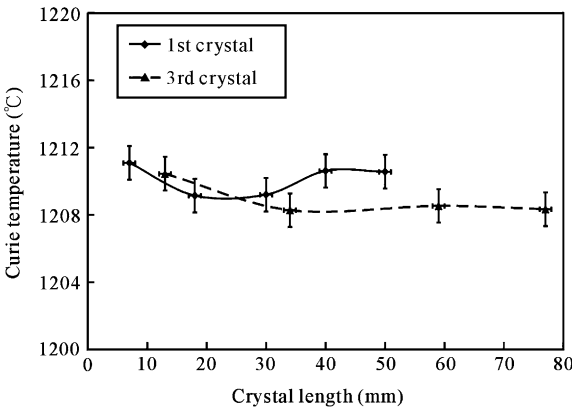

Fig. 7. Axial distributions of the Curie temperature of the 1st and the 3rd crystals.

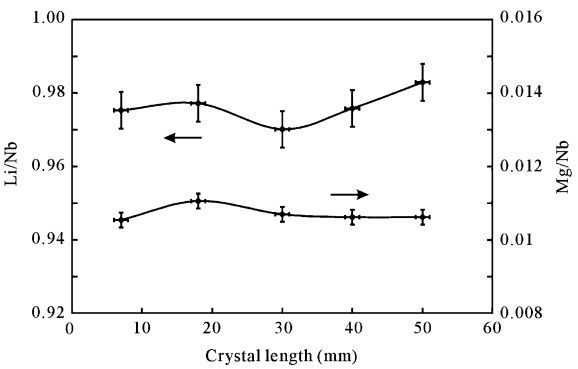

Fig. 8. Axial distributions of the Li/Nb and Mg/Nb ratios of the 1st crystal.

assume Mg ions could replace Li sites [25], i.e., $Mg_{0.01}Li_{1-0.02}NbO_3$, the best Li/Nb ratio is about 98%. Therefore, taking the sensitivity of the chemical analyses into account, we believe that the Li/Nb ratios of the first two crystals should be satisfactory.

Although the zone length could change during growth, the change in the zone composition was found to be small. In fact, based on a simple mass balance calculation, if the zone length changed from 4.5 to 5.5 cm, the Li/Nb ratio in the solution zone would change only from 1.5 (60 mol% Li_2O) to 1.435 (59 mol% Li_2O) due to the dissolution of the feed. This estimate was consistent with the measured ones. Furthermore, because the segregation coefficient of MgO is very near unity [16], we did not observe much MgO difference among the crystals. Therefore, the non-uniformity based on the previous measurements was mainly due to the Li/Nb ratio. However, such a small difference could not be determined accurately enough by the chemical analyses. Nevertheless, to further improve the uniformity, the crystal lifting speed should be varied according to the amount of the crystal pulled. Moreover, a longer feed length is preferred for keeping the position of the melt/feed interface constant.

4. Conclusions

SLN single crystals with 1 mol% MgO doping were successfully grown by using the ZLCz technique. With the inner crucible and the automatic diameter control, the grown crystals were found to be inclusion-free and exhibited good uniformity. After three growth experiments, the composition of the solution zone did not change much. As a result, the ICP-measured Li/Nb ratio was close to the stoichiometric limit (0.98), and the MgO distribution was quite uniform at 1.07%. Nevertheless, the optical and the Curie temperature measurements still showed some variations especially for the 3rd crystal. The Li/Nb ratio in the 3rd crystal was believed to be lower due to the longer solution zone. Still, all the measured values were consistent with the published ones. Therefore, we could conclude that the ZLCz technique should be a promising method for the growth of high-quality SLN single crystals.

Acknowledgments

This work was mainly supported by the National Science Council of Taiwan and Sino-American Silicon Products Inc. Partial support from National Taiwan University, and the Material Science Laboratory of the Industrial Technology Research Institute is also acknowledged. Useful comments from Prof. D.T.J. Hurle on the upper weighting system at the beginning of the system design are highly appreciated.

References

[1] G. Assanto, I. Torelli, Opt. Commun. 119 (1995) 143.
[2] H. Kang, C.X. Yang, G.G. Mu, Z.K. Wu, Opt. Lett. 15 (1990) 637.
[3] J.F. Heanue, M.C. Bashaw, L. Hesselink, Science 265 (1994) 749.
[4] L.E. Myers, G.D. Miller, R.C. Eckardt, M.M. Fejer, R.L. Byer, Opt. Lett. 20 (1995) 52.
[5] P.F. Bordui, R.G. Norwood, C.D. Bird, G.D. Calvert, J. Crystal Growth 113 (1991) 61.
[6] M. Nakamura, S. Higuchi, S. Takekawa, K. Terabe, Y. Furukawa, K. Kitamura, Jpn. J. Appl. Phys. 41 (2002) L49.
[7] V. Gopalan, T.E. Mttchell, Y. Furukawa, K. Kitamura, Appl. Phys. Lett. 72 (16) (1998) 1981.
[8] Y. Furukawa, K. Kitamura, S. Takekawa, K. Niwa, H. Hatano, J. Intell. Mater. Syst. Struct. 10 (1999) 470.
[9] G.I. Malovichko, V.G. Grachev, E.P. Kokanyan, O.F. Schirmer, K. Betzler, B. Gather, F. Jermann, S. Klauer, U. Schlarb, M. Wöhlecke, Appl. Phys. A 56 (1993) 103.
[10] S. Solanki, T.C. Chong, X. Xu, J. Crystal Growth 250 (2003) 134.
[11] K. Kitamura, J.K. Yamamoto, N. Iyi, S. Kimura, T. Hayashi, J. Crystal Growth 116 (1992) 327.
[12] Y. Furukawa, M. Sato, K. Kitamura, F. Nitanda, J. Crystal Growth 128 (1993) 909.
[13] S. Kan, M. Sakamoto, Y. Okano, K. Hoshikawa, T. Fukuda, J. Crystal Growth 128 (1993) 915.
[14] C.W. Lan, H.J. Chen, C.B. Tsai, J. Crystal Growth 245 (2002) 56.
[15] K. Kitamura, Y. Furukawa, S. Takekawa, S. Kimura, US Patent no. 6673330, 2004.
[16] K. Niwa, Y. Furukawa, S. Takekawa, K. Kitamura, J. Crystal Growth 208 (2000) 493.

[17] Y.L. Chen, J.P. Wen, Y.F. Kong, S.L. Chen, W.L. Zhang, J.J. Xu, G.Y. Zhang, J. Crystal Growth 242 (2002) 400.
[18] Y. Furukawa, K. Kitamura, S. Takekawa, K. Niwa, H. Hatano, Opt. Lett. 23 (1998) 1892.
[19] H. Wang, Y. Hang, L. Zhang, J. Xu, M. He, S. Zhu, Y. Zhu, S. Zhou, J. Crystal Growth 262 (2004) 313.
[20] S.I. Bae, J. Ichikawa, K. Shimamura, H. Onodera, T. Fukuda, J. Crystal Growth 180 (1997) 94.
[21] A. Yamada, H. Tamada, M. Saitoh, J. Crystal Growth 132 (1993) 48.
[22] D.H. Jundt, M.M. Fejer, R.L. Byer, IEEE J. Quantum Electron. EQ-26 (1990) 135.
[23] H.M. O'Bryan, P.K. Gallagher, C.D. Brandle, J. Amer. Ceram. Soc. 68 (1985) 493.
[24] Y. Furukawa, K. Kitamura, S. Takekawa, K. Niwa, Y. Yajima, N. Iyi, I. Mnushkina, P. Guggenheim, J.M. Martin, J. Crystal Growth 211 (2000) 230.
[25] N. Iyi, K. Kitamura, Y. Yajima, S. Kimura, Y. Furukawa, M. Sato, J. Solid State Chem. 118 (1995) 148.